CROSSED MOLECULAR BEAM STUDY OF COLLISION-INDUCED
DISSOCIATION OF ALKALI HALIDES*

F.P. TULLY, Y.T. LEE** and R.S. BERRY

*The James Franck Institute and Department of Chemistry,
The University of Chicago, Chicago, Illinois 60637, USA*

The collision-induced dissociation process of alkali halides to ion pairs by high energy Xe was studied by crossed molecular beam method. The dependence of the dissociation cross section on relative kinetic energy and alkali halide internal energy was investigated.

Recent studies by Berry et al. [1,2] of collisional dissociation of alkali halides by shock-heated argon have shown that, in vibrationally-equilibrated gases, some alkali halides (all cesium, rubidium and potassium salts except RbI and KI) dissociate completely to ion pairs, although dissociation to neutral atoms requires less energy. An expression for the branching ratio for the different dissociation products (atomic or ionic) has been postulated for these systems.

The present experiments utilize the crossed molecular beam method for further investigation of the more elementary process of dissociation of CsI, CsBr and RbI to ion pairs by single collisions with high energy xenon atoms***. Since both the relative kinetic energy and internal energy of the reactants can be precisely controlled in a crossed molecular beam experiment, the dependence of the dissociation cross section on relative kinetic energy and alkali halide internal energy has been measured for collision energies up to 6 eV and alkali halide temperatures ranging from 1150 °K to 1650 °K. Crude energy analysis of the ions produced by these single collisions also reveals interesting dynamical features of collision-induced dissociation.

The schematics of the experimental arrangement are shown in fig. 1a. Fast Xe is produced by the seeded supersonic beam technique [5]. A mixture of 1% Xe and 99% H_2 is expanded through a 0.1 mm diameter nozzle. The energy of the Xe atom is controlled by the nozzle (oven) temperature, the upper limit of which is 1000 °C. With a typical operating source pressure of 1650 to 2250 torr the pressures in the nozzle-skimmer and skimmer-collimator chambers are in the mid 10^{-4} torr and 10^{-6} torr ranges. These regions are pumped differentially by 10 inch and 4 inch oil diffusion pumps. For sufficiently high source pressure, the isentropic expansion will produce xenon and hydrogen of the same terminal velocity which is given by $\mu = (5kT/m)^{1/2}$ ‡ where $m = 0.01 M_{Xe} + 0.99 M_{H_2} = 3.29$ and T is the nozzle temperature. The Xe energy obtained, $(5/2)(M_{Xe}/m)kT$, is thus a factor of M_{Xe}/m (≈ 40) larger than that which would be obtained by expanding pure Xe. When the nozzle temperature is 1000 °C, the Xe atom lab energy is 11.0 eV. Other nice features of the seeded supersonic beam technique are the increase in Xe center-line concentration from an initial 1% mixture and the narrow velocity distribution typical of supersonic nozzle beams. The width of the Xe beam is 2.5°.

The effusive alkali halide beam is from a double oven located in another chamber maintained at high 10^{-7} torr by a 4 inch diffusion pump. A lower stainless steel oven heated by alumina-insulated tantalum wire controls the vapor pressure of the alkali halide. The alkali halide vapor

---

‡ This terminal velocity is characteristic of seeded beam expansions in carrier gases of specific heat ratio 5/3. For hydrogen as the carrier gas, expansion yields lower terminal velocities than those predicted for diatomic carrier gases ($C_p/C_v = 7/5$), an observation attributed to hydrogen's very slow rotational relaxation. See ref. [4].
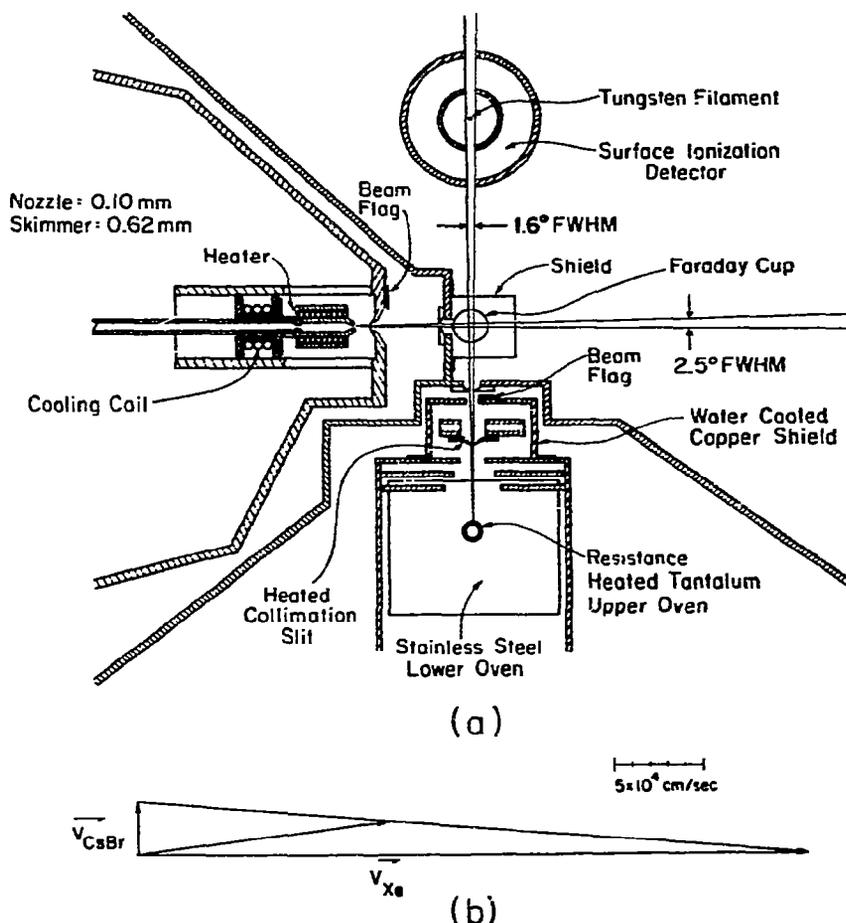
Fig. 1. a) Schematic diagram of experimental arrangement. b) Newton diagram for a typical experiment.

then flows into a resistance-heated upper oven made of a 6.35 mm diameter tantalum tube which is 9.5 cm long and 0.5 mm thick. The rectangular slit of the upper oven is 0.76 mm by 3.05 mm. A stainless steel heating block with alumina insulated tantalum heaters is mounted on the upper part of the tantalum tube in order to achieve homogeneous heating along the tube and to maintain a maximum in temperature at the slit. The temperature at the slit is measured by an optical pyrometer and the beam is collimated to 1.6° by two defining slits. Four successive water cooled copper plates located between the oven and the differential pumping wall provide most of the trapping of the alkali halide. Beam intensity is measured by surface ionization on a tungsten filament.

The beams are crossed at 90 degrees in the main chamber which is maintained at about 10^{-7} torr by a 10 inch diffusion pump. The beam in-

tensities at the collision center are approximately 6×10^{16} molecules/cm^{2}sec for Xe and 6×10^{14} molecules/cm^{2}sec for the alkali halide. The ions produced in the collision are collected by means of a repeller plate-Faraday cup arrangement. Both positive and negative ions currents may be measured by changing the polarity of the repeller plate. The repeller plate and the cylindrically symmetric Faraday cup are located above and below the collision center respectively and parallel to the beam plane.

The Newton diagram for a typical experiment is shown in fig. 1b. Since the Xe velocity is more than 10 times that of the alkali halide, the magnitude of the nominal relative velocity is essentially the same (within 1%) as that of the Xe velocity and it has a fwhm velocity spread of less than 10%, mainly determined by the distribution in xenon velocities. The maxwellian velocity distribution of the slow alkali halide does

not further contribute to the spread in relative kinetic energy, and consequently the velocity of the alkali halide beam was not selected.

Fig. 2 gives curves of total ion current as a function of center of mass collision energy. The dissociation thresholds extrapolated from these curves are 4.35 ± 0.15 eV, 4.42 ± 0.20 eV, and 4.40 ± 0.35 eV for CsI, CsBr, and RbI respectively. These are in fair agreement with the accepted values of 4.37 eV, 4.68 eV, and 4.41 eV for dissociation to the ionic limit (compared with 3.54 eV, 4.15 eV, and 3.30 eV, for dissociation to the atomic limit) [5]. In any event, threshold energies for dissociation determined by extrapolating curves for monoenergetic collisions must represent upper limits for the true dissociation energies. However, the uncertainty of collision energies in this experiment, associated with the assumptions regarding the seeded beam, are probably greater than observed discrepancies. The total cross sections for collision-induced dissociation of CsI and CsBr at energies of 5.4 eV are estimated to be more than 10 $\mathring{A}^2$, the dissociation cross section for CsI being somewhat larger than that of CsBr. The surprisingly large cross sections of these processes indicate both a rather high dissociation efficiency for collisions with relatively large impact parameter and the sufficiency of kinetic energy to dissociate alkali halides of low internal excitation provided the kinetic energy is somewhat larger than threshold. The sharp threshold behavior of CsI ($M_{Cs}/M_I \approx 1$) can be contrasted
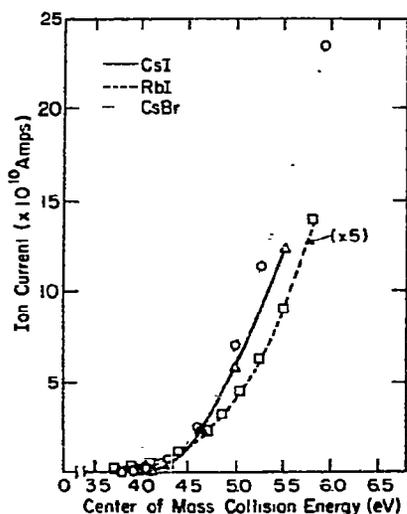

Fig. 2. Dependence of total ion current on center of mass collision energy for CsI, CsBr and RbI.

with the slower rise of both CsBr and RbI ($M_{Br}/M_{Cs} \approx M_{Rb}/M_I \approx 0.6$). The effect of differences in the alkali halide atomic mass ratio is also observed in the energy distributions of the dissociated ions.

If the Xe (H_2) source temperature is kept constant while the alkali halide source temperature is varied, a large change is effected in the alkali halide internal energy without appreciably changing the relative kinetic energy of the collision process.

In fig. 3a, the relative efficiency of ion production is plotted as a function of CsBr temperature at two different collision energies. The ordinate in fig. 3a is Cs^+ current divided by CsBr number density, a quotient proportional to the dissociation cross section for constant Xe flux. If the collision energy is near the dissociation threshold, the cross section shows a pronounced internal energy dependence. When the CsBr temperature is increased from 1150 °K to 1650 °K, an average total energy increase of only 1.34 kcal/mole, the ratio of the cross sections over this range is 3.32. But, for the same total energy, if the kinetic energy is increased by 1.34 kcal/mole while the alkali halide temperature is held at 1150 °K the cross section only increases by 6%. Therefore, as expected, it is seen that for collision energies near threshold, internal energy is more effective than kinetic energy in producing dissociation. This conclusion is in general agreement with that obtained for some endothermic chemical reactions near threshold by applying microscopic reversibility to the detailed information provided by chemiluminescence experiments on the reverse exothermic reactions [6,7]. In these endothermic chemical reactions it has been concluded that energy in a vibrational mode is, for a given total energy, most productive in effecting reaction.

When the collision energy is raised to about 1.5 eV above threshold, the cross sections increase one to two orders of magnitude, but, at these higher energies, when the alkali halide temperature is increased from 1150 °K to 1650 °K, the cross section increases only by a factor of 0.23. This indicates that as the kinetic energy increases appreciably beyond threshold, the dissociation proceeds very effectively regardless of the alkali halide internal energy.

Fig. 3a indicates that the dissociation cross section for threshold collision energy is an exponential function of CsBr temperature, $\sigma(T) = Ae^{BT}$, where A and B are constants. If we define the specific dissociation cross section for a given internal energy E_I as $\sigma(E_I)$, then at this
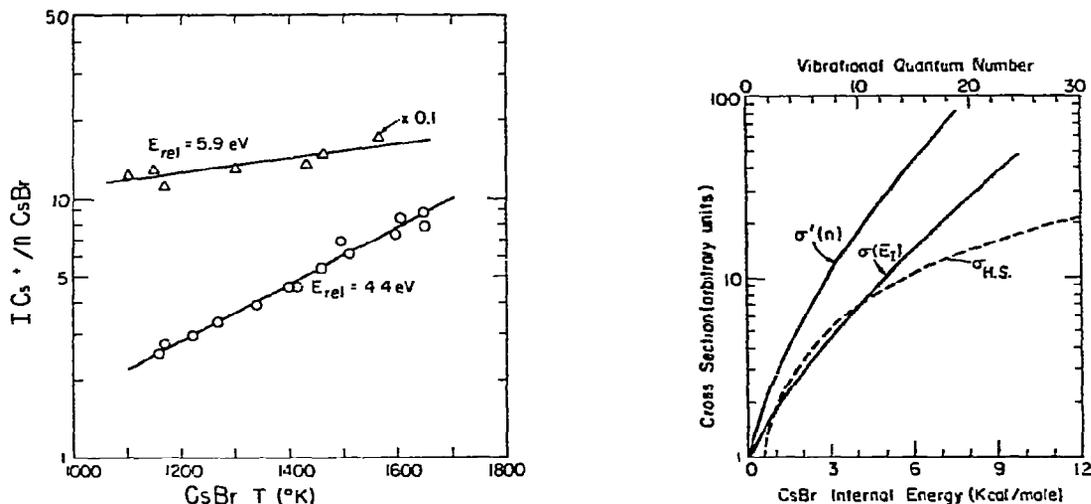
Fig. 3. a) Relative efficiency of ion production as a function of CsBr temperature for two different collision energies. b) Dissociation cross sections as function of internal CsBr energy and vibrational quantum number calculated from data shown in fig. 3a. The hard sphere endothermic reaction cross section is also shown.

collision energy the observed $\sigma(T)$ has the following relation

$$\sigma(T) = A e^{BT} = \int_0^\infty \sigma(E_I) \, P(E_I) \, dE_I, \qquad (1)$$

where

$$P(E_I) = \frac{E_I e^{-\beta E_I}}{\int_0^\infty E_I e^{-\beta E_I} dE_I} \quad \text{and} \quad \beta = \frac{1}{kT_{CsBr}}.$$

Applying an inverse Laplace transform to (1), and using the best exponential parameters

$$L^{-1}\left\{ \frac{A e^{B/k\beta}}{\beta^2} \right\} = E_I \, \sigma(E_I),$$

$\sigma(E_I)$ can be unfolded as

$$\sigma(E_I) = A' E_I^{-1/2} \, I_1(2.267 \, E_I^{1/2})$$

for E_I in kcal/mole.

I_1 is a modified Bessel function of 1st order. A plot of $\sigma(E_I)$ versus E_I is shown in fig. 3b. Similarly, if we assume that the rotational energy of CsBr does not contribute to the dissociation and define the specific dissociation cross section for a given vibrational state, $v = n$, as $\sigma'(n)$, then the same unfolding procedure can be used. Considering n as a continuous variable and using the classical function, we obtain

$$\sigma'(n) = A'' I_0 (1.43 \, n^{1/2}).$$

I_0 is a zeroth order modified Bessel function; $\sigma'(n)$ is also shown in fig. 3b. The cross sections $\sigma(E_I)$ and $\sigma'(n)$ are normalized to the same value for zero internal energy and are plotted on the same energy scale. The hard sphere endothermic reactive cross section

$$\sigma = \pi d^2 (1 - D/E)$$

is also shown in fig. 3b, where E is the kinetic energy of relative motion and $D = D_0 - E_I$ is the effective dissociation energy for a given internal energy E_I.

The Faraday cup is not only used to collect all the positive or negative ions, but also serves as a crude energy analyzer by virtue of its adjustable repeller voltage. Fig. 4 shows ion current as a function of repeller voltage for collision energies slightly above threshold and a few eV above threshold. Approximate laboratory energy distributions can be obtained from the slopes of these curves, since the ions produced move nearly parallel to beam plane due to their large in-plane velocity of center of mass as compared with their relative velocity, and thus the voltage required to bend an ion trajectory to the Faraday cup is approximately proportional to the laboratory energy of the ion. At collision energies near dissociation threshold almost all the available energy goes into the dissociation process and the product ions can be expected to have only small recoil velocities with respect to the center of mass. The lab velocities of these low recoil will then be approximately equal to the velocity
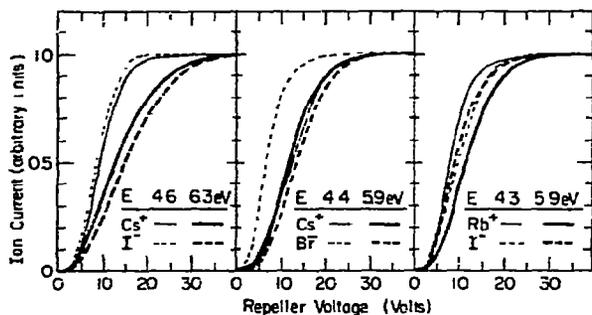
Fig. 4. Dependence of positive and negative ion currents collected in the Faraday Cup on the repeller plate voltage for CsI, CsBr and RbI at two different collision energies.

of the center of mass, C, and the lab energies will be proportional to the ion masses. It is seen from fig. 4 that at threshold energies the heavier ions require higher collection voltages than the light ions, an observation consistent with low recoil velocities. At collision energies a few eV above threshold, where enough energy is available so that recoil velocities need not be small, it is observed that the lighter ion has higher lab energy. The smooth energy distributions and the large total cross sections characteristic of these high energy collisions imply that non-collinear collisions are much more important than collinear collisions in the dissociation process, since collision-induced dissociation caused mainly by collinear collisions would produce two distinct peaks in the energy distribution for each ion. Also, after establishing the effective field strength from the threshold energy experiments where the ion lab energies are known to be $\approx \frac{1}{2} MC^2$, calculation of the lab velocities for the high collision energy experiments show $|V_{light}| > |C| > V_{heavy}|$ in all cases. This observation suggests that Xe on light atom is more effective in inducing dissociation than Xe on heavy atom.

Recent exact classical calculations by Kelley and Wolfsberg [8] on collisional energy transfer to diatomic molecules with a rotational and a vibrational degree of freedom have shown that the non-collinear collisions are more impulsive than collinear collisions and consequently are more efficient in exciting the vibrational mode of motion. Their calculations also indicate that an atom colliding initially with the light end of the molecule gives more efficient energy transfer from the translational degree of freedom to the vibrational and rotational degrees of freedom than an atom colliding initially with the heavy end of the molecule. This conclusion is in general qualitative agreement with our observations.

The large cross sections observed in these experiments could be due mainly to the nature of alkali halide chemical bonding. Since the attractive part of the alkali halide potential is dominated by the coulombic $1/r$ term, while the centrifugal potential varies as $1/r^2$, there is no centrifugal barrier to alkali halide dissociation. This condition is in contrast to that of covalently bonding molecules where centrifugal barriers might considerably affect the collision-induced dissociation cross section for similar collision and dissociation energies. More detailed studies which also involve other alkali halides are under way in our laboratory.

REFERENCES

[1] R. S. Berry, T. Cernoch, M. Coplan and J. J. Ewing, J. Chem. Phys. 49 (1968) 127.
[2] J. J. Ewing, R. Milstein and R. S. Berry, J. Chem. Phys., to be published.
[3] J. B. Anderson, Entropie 18 (1967) 33; N. Abuaf, J. B. Anderson, R. P. Andres, J. B. Ferr and D. G. H. Marsden, Science 155 (1967) 997.
[4] N. Abuaf, Ph. D. thesis, Princeton University (1966).
[5] L. Brewer and E. Brackett, Chem. Rev. 61 (1961) 425; Y. P. Varshni and R. C. Shukla, J. Mol. Spectry. 16 (1965) 63.
[6] R. G. Anlauf, D. H. Maylotte, J. C. Polanyi and R. B. Bernstein, J. Chem. Phys. 51 (1969) 5716.
[7] J. C. Polanyi and D. C. Tardy, J. Chem. Phys. 51 (1969) 5717.
[8] J. D. Kelley and M. Wolfsberg, J. Chem. Phys. 53 (1970) 2967.